

Nanoscale Dichotomy of Ti 3d Carriers Mediating the Ferromagnetism in Co:TiO₂ Anatase Thin Films

T. Ohtsuki,¹ A. Chainani,¹ R. Eguchi,^{1,2} M. Matsunami,^{1,2} Y. Takata,¹ M. Taguchi,¹ Y. Nishino,¹
K. Tamasaku,¹ M. Yabashi,³ T. Ishikawa,¹ M. Oura,¹ Y. Senba,³ H. Ohashi,³ and S. Shin^{1,2}

¹*RIKEN SPring-8 Center, Sayo-cho, Sayo-gun, Hyogo 679-5198, Japan*

²*Institute for Solid State Physics, The University of Tokyo, Kashiwa, Chiba 277-8581, Japan*

³*JASRI/SPring-8, Sayo-cho, Sayo-gun, Hyogo 679-5198, Japan*

(Dated: May 22, 2018)

We study the surface and bulk electronic structure of the room-temperature ferromagnet Co:TiO₂ anatase films using soft and hard x-ray photoemission spectroscopy with probe sensitivities of ~ 1 nm and ~ 10 nm, respectively. We obtain direct evidence of metallic Ti³⁺ states in the bulk, which get suppressed to give a surface semiconductor, thus indicating a surface-bulk dichotomy. X-ray absorption and high-sensitivity resonant photoemission spectroscopy reveal Ti³⁺ electrons at the Fermi level (E_F) and high-spin Co²⁺ electrons occurring away from E_F . The results show the importance of the charge neutrality condition: $\text{Co}^{2+} + \text{V}_O^{2-} + 2\text{Ti}^{4+} \leftrightarrow \text{Co}^{2+} + 2\text{Ti}^{3+}$ (V_O is oxygen vacancy), which gives rise to the elusive Ti 3d carriers mediating ferromagnetism via the Co 3d-O 2p-Ti 3d exchange interaction pathway of the occupied orbitals.

PACS numbers: 79.60.-i, 73.20.-r, 75.50.-y

Dilute ferromagnetic oxides have been at the forefront of a paradigm shift in the search for spintronics and magneto-optic device materials [1–6]. However, for achieving reliable thin-film device performance, it is necessary to ensure the surface and bulk electronic properties of candidate materials. This is particularly true for high Curie-temperature oxide ferromagnets for spintronics which can be synthesized only in thin film form, such as Co:TiO₂ [2], Mn:ZnO [3], Cr:In₂O₃ [4], etc. The main question that still remains enigmatic: What changes drive the long-range coupling of local moments in an insulating parent? The pre-runners, namely, dilute magnetic semiconductors (DMSs) which consisted of magnetic 3d transition metal (TM) ions doped in III-V and II-VI compounds, showed a Curie-temperature (T_c) well-below room temperature e.g. InMnAs, GaMnAs, Zn-CrTe, etc [7–9]. Theoretical studies of carrier-mediated ferromagnetism played a pivotal role in predicting high- T_c ferromagnets in the dilute substitution limit [10]. The spin-charge degrees of freedom and the anisotropic character of the dopant TM d -orbitals results in a directional dependence of exchange energies and T_c 's of upto 170 K [11, 12]. The limitation of T_c 's significantly lower than room temperature motivated studies on alternative parents, like oxides and nitrides. The discovery of ferromagnetism in Co-doped TiO₂ (Co:TiO₂), with a T_c exceeding 300 K [2], was crucial in expanding the field to oxides, leading to a rapid increase of new materials and phenomena arising from a synergetic marriage of semiconductor physics and strongly correlated systems.

From extensive magnetic and transport studies, it is now well-accepted that Co:TiO₂ films grown in a reducing environment or annealed in vacuum result in Co segregation [13, 14], while films grown in an oxidizing condition are intrinsically ferromagnetic with high

spin Co²⁺ [15, 16]. While initial x-ray magnetic circular dichroism (XMCD) measurements and annealing in vacuum concluded that the ferromagnetism was extrinsic due to segregated Co metal clusters [14], subsequent XMCD studies showed intrinsic ferromagnetism in Co:TiO₂ grown in oxidizing conditions [17]. A soft x-ray surface-sensitive photoemission study indicated the importance of exchange interaction between the occupied Co t_{2g} and conduction band Ti t_{2g} states [18], but concluded that anatase Co:TiO₂ are wide band gap semiconductors. Recent experimental studies have emphasized the importance of oxygen vacancies (V_O) in Co:TiO₂ [15, 19]. The above results are consistently explained by the theoretical model of a hydrogenic spin-split donor-impurity band interacting via ferromagnetic exchange with the localized spins to realize high- T_c ferromagnetism [20]. However, the experimental results are still not conclusive about the origin of the donor band: whether it is derived from shallow oxygen vacancies or cation vacancies, singly occupied vacancies or doubly occupied vacancies, or due to Co²⁺- V_O complexes [19]. This is a critical missing input to the mechanism of ferromagnetism in Co:TiO₂. In this work, we address this issue using surface and bulk-sensitive [21] photoemission spectroscopy (PES), x-ray absorption (XAS) and high-sensitivity resonant (R) PES. Our results unambiguously show that the carriers are the occupied Ti³⁺ 3d electrons, a possibility completely neglected to date, and these electrons exhibit a nanoscale surface-bulk dichotomy of the electronic structure of Co:TiO₂ which would play a crucial role in real device applications.

Co:TiO₂ thin films were fabricated on SrTiO₃(100) single crystal substrates by pulsed laser deposition (PLD) method. A KrF excimer laser (Lambda Physik, $\lambda = 248$ nm) was used to ablate sintered pellet target

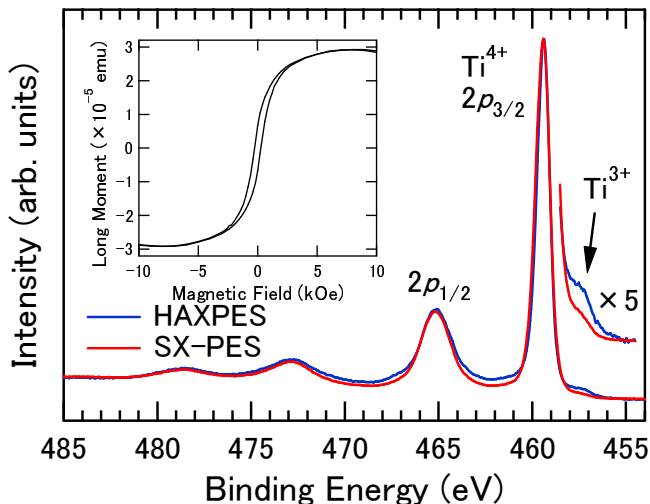


FIG. 1. Ti $2p$ core-level PES of Co:TiO₂ thin film by HAXPES (blue) and SX-PES (red), respectively. HAXPES and SX-PES were measured with photon energies of 7940 eV and 1200 eV, respectively. The close up view of the spectra ($\times 5$) at lower binding energy side of main Ti $2p_{3/2}$ peak is shown together. Ti³⁺ components can be clearly recognized. The inset is the magnetization vs. magnetic field curve of the same film measured at room temperature. The observed hysteresis confirms the room temperature ferromagnetism in this Co:TiO₂ thin film.

(Ti_{0.95}Co_{0.05}O₂). The laser fluence and repetition rate were set to 1.2 J/cm²/pulse and 3 Hz, respectively. During deposition, the oxygen partial pressure ($P(O_2)$) and substrate temperature were fixed at 1×10^{-6} Torr and 650 °C, respectively. X-ray diffraction (XRD) measurements confirmed the epitaxial growth of these films in (001)-oriented anatase phase (See [22] for details of characterization), which also showed ferromagnetism at room temperature [6].

Hard x-ray(HAX)-PES measurements were carried out at undulator beamline BL29XU at SPring-8 using a photon energy of 7940 eV and Gammadata-Scienta R4000-10kV electron energy analyzer [21]. The total energy resolution was set to 250 meV. The soft x-ray(SX)-PES measurements were carried out at undulator beamline BL17SU of SPring-8. The PES spectra were obtained using a Gammadata-Scienta SES-2002 electron energy analyzer. The total energy resolutions were set to 240 meV with $h\nu = 1200$ eV and 230 meV for RPES measurements, respectively. The Fermi level (E_F) of the samples was referred to that of an Au film deposited on the sample substrate. The XAS spectra were taken in the total electron yield mode and were calibrated by measuring Au $4f$ PES peak excited with first- and second-order light. All the measurements were performed at room temperature.

Figure 1 shows the Ti $2p$ core-level spectra of Co(5 at%):TiO₂ thin films grown epitaxially on a SrTiO₃(100) substrates. The inset shows the hysteresis at 300 K con-

firning the ferromagnetism [22]. The Ti $2p$ core-level spectra measured with SX-PES ($h\nu = 1200$ eV) and HAXPES ($h\nu = 7940$ eV) show a main Ti $2p_{3/2}$ peak at 459.4 eV and $2p_{1/2}$ peak at 465.2 eV due to Ti⁴⁺ states, accompanied by charge-transfer satellites at 13 eV higher binding energies [23]. In addition, a fine structure is observed at 1.8 eV lower binding energy to the main peak. We plot the SX-PES and HAXPES on an enlarged ($\times 5$) scale and normalized to the main peak intensity (inset Fig. 1), which clearly shows that this feature is enhanced in the HAXPES data compared to SX-PES. This feature is not observed in the case of stoichiometric Ti⁴⁺ (d^0 state) titanates, but shows up in reduced/electron-doped titanates indicative of Ti³⁺ states [24, 25]. A similar behaviour was recently found for the 2D-electron gas at SrTiO₃-LaAlO₃ interface using HAXPES [26]. The present results indicate that Ti³⁺ components in Co:TiO₂ thin films are clearly present in bulk-sensitive HAXPES with a probing depth of ~ 10 nm and they are suppressed in the top 1-2 nm, as probed by surface sensitive SX-PES. For δ oxygen vacancies, 2δ electrons are introduced into valence band states consisting of Ti $3d$ and O $2p$ electrons [27]. In addition, if Co is doped as Co²⁺ (as confirmed below), oxygen defects are also necessary to keep charge neutrality. If the carriers are trapped, these are described as Co²⁺ + V_O²⁻ complexes [19]. However, our core-level O $1s$ spectra show a clean single peak [22] but with a small shift in binding energies, suggestive of negligible role of oxygen vacancies. Taken together with the presence of Ti³⁺, it indicates the following charge neutral transformation, Co²⁺ + V_O²⁻ + 2Ti⁴⁺ \leftrightarrow Co²⁺ + 2Ti³⁺. This is consistent with no changes in Co co-ordination using extended x-ray absorption fine structure (EXAFS), suggesting that the defects are mobile and not localized to the first co-ordination shell of Co²⁺ ions [15].

In order to confirm Ti³⁺, we measured the valence band spectra with SX-PES and HAXPES (Fig. 2). Non-doped anatase TiO₂ is a wide-gap semiconductor with a band gap of 3.2 eV [28], and the observed gap in Fig. 2 seems to confirm it (green arrow in Fig. 2). This indicates that E_F is pinned at the bottom of the conduction band. However, in the inset of Fig. 2, we plot high signal-to-noise ratio near- E_F data on an enlarged ($\times 85$) y-scale, and it clearly shows in-gap states. More importantly, the spectra show a depletion of states at E_F for the SX-PES data while the HAXPES data shows a clear Fermi-edge step. This indicates a nanoscale surface-semiconductor : bulk-metal dichotomy. Next, we investigate the electronic character of the in-gap region in detail, using Co $2p$ - $3d$ and Ti $2p$ - $3d$ XAS and RPES measurements which provides unoccupied and occupied element/site-projected and orbital-selective $3d$ partial density of states (DOS), respectively.

Figure 3(a) shows the experimental XAS spectrum of anatase Co:TiO₂ at the Co L_3 -edge, compared with

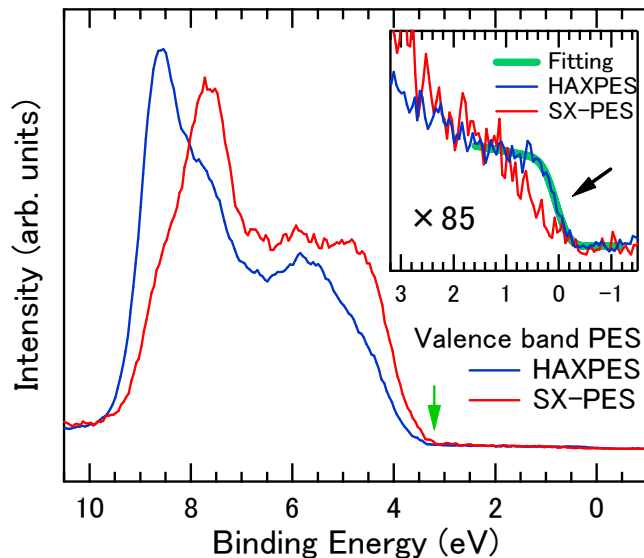


FIG. 2. Valence band PES of Co:TiO₂ thin film by HAXPES (blue) and SX-PES (red). The spectra are normalized by the peak area. A green arrow indicates the position of reported band-gap value [28]. The inset is the enlargement of the spectra ($\times 85$) near- E_F . A green line is the fitting curve of HAXPES spectrum. HAXPES spectrum clearly shows Fermi-edge step (marked by black arrow).

the theoretically calculated low-spin and high-spin Co²⁺ spectrum of Co ions [22]. The rich structure found in the experimental spectrum of Fig. 3(a) shows very good correspondence with the calculated high-spin Co²⁺ spectrum and also rules out the low spin Co²⁺ configuration. It is also quite similar to that of rutile Co:TiO₂ [17]. The results thus confirm a high-spin Co²⁺ ion substituted in the Ti⁴⁺ site for Co:TiO₂.

Figure 3(b) shows the Co $2p$ - $3d$ valence band RPES of Co:TiO₂ obtained with photon energies A-H marked in Fig. 3(a). A comparison of the off-resonance spectrum (A) with on-resonance spectra (B-H) indicates that the spectral changes observed at ~ 1 to ~ 3.5 eV binding energy corresponds to the new Co $3d$ states obtained in the gap, while changes in the O $2p$ states result from hybridization changes accompanying the doping. From Fig. 3(b), we also verify that the Co $3d$ states are not located at E_F , thus indicative of localized Co $3d$ electrons.

Figure 4 shows the Ti $2p$ - $3d$ XAS and RPES of Co:TiO₂ thin films measured to clarify the Ti $3d$ states in the electronic structure. The wide energy scale RPES spectra are shown in Fig. 4(a) while the near- E_F in-gap region spectra are shown in Fig. 4(b). The photoemission intensities are normalized by photon flux and the high-sensitivity near- E_F spectra are magnified ($\times 160$) in order to characterize the spectral features. Off-resonant spectrum ($h\nu = 454$ eV) shows no striking changes from the valence band PES shown in Fig. 2. In contrast, the on-resonant spectra show two clear features: a weak fea-

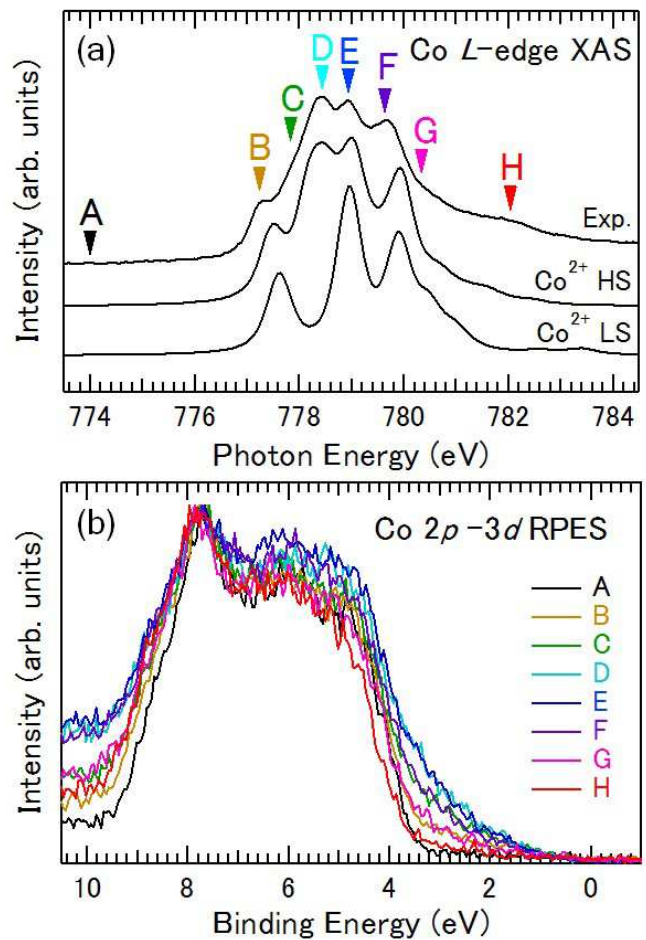


FIG. 3. (a) The XAS spectra of Co:TiO₂ thin film near Co L_3 -edge. The labels Exp., Co²⁺ HS, and Co²⁺ LS correspond to the experimental data, calculation of divalent high-spin state, and divalent low-spin state, respectively. (b) RPES spectra by Co $2p$ - $3d$ resonance. The intensities of RPES spectra are normalized by peak height. The labels A-H correspond to excitation photon energies as marked in (a).

ture at E_F and another higher intensity feature at ~ 1 eV binding energy, arising from coherent and incoherent features of d^1 Ti³⁺ states in the Mott-Hubbard picture of strongly correlated electrons [29]. Interestingly, we have plotted the integrated intensity of the in-gap states as a function of incident photon energy in Fig. 4(c), and at first glance, it shows no correspondence with sharp features in the Ti $2p$ - $3d$ XAS spectrum. However, a comparison with the Ti $2p$ - $3d$ XAS of Ti₂O₃ (Ti³⁺) single crystal fractured in vacuum (blue line in Fig. 4(c) [30]) shows a very good match with the peak at 459.2 eV. Hence, the resonant enhancement around 459 eV is due to the Ti³⁺ component in Co:TiO₂.

Thus, while the core level and valence band spectra of Figs. 1 and 2 clearly show Ti³⁺ states, the RPES results show that the in-gap states (inset of Fig. 2) are actually derived from Co $3d$ and Ti $3d$ states. The magnetic Co

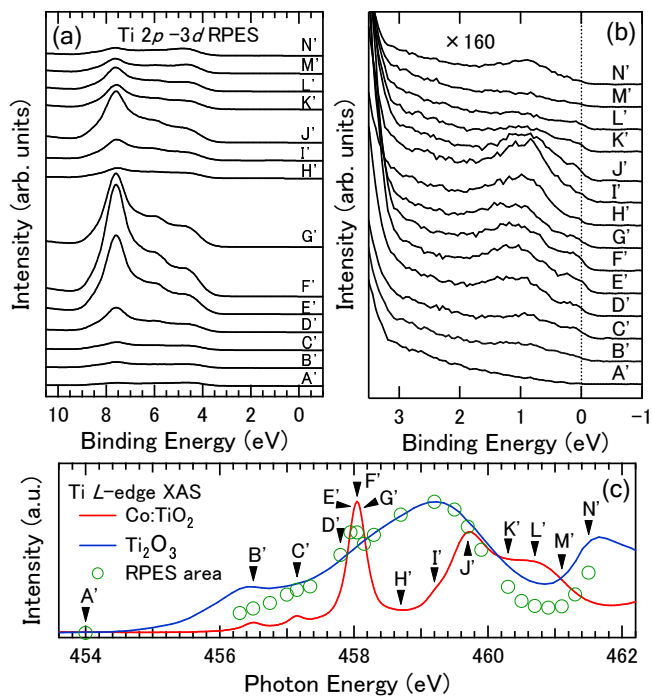


FIG. 4. (a) Ti $2p$ - $3d$ RPES spectra of Co:TiO₂ thin film plotted in wide region. The photoemission intensities are normalized by photon flux. (b) The enlarged scale ($\times 160$) plot of (a) near- E_F . The labels A'-H' correspond to excitation photon energies as marked in (c). (c) The XAS spectra of Co:TiO₂ thin film (red) and Ti₂O₃ single crystal [30] (blue) around Ti L_3 -edge. The integrated peak areas from -0.5 to 2.5 eV in (b) are also plotted by green open circle.

$3d$ states are spread over a wide energy range from ~ 1 to 3.5 eV, while Ti $3d$ states which provide carriers occur from E_F to about 2 eV. Consequently, the partial DOS of Co $3d$ and Ti $3d$ overlap significantly and would be well-hybridized, constituting a Co $3d$ -O $2p$ -Ti $3d$ ferromagnetic exchange pathway responsible for a spin-charge coupled nanoscale dichotomy. The results conclusively indicate that the ferromagnetism of Co:TiO₂ is explained by a carrier-induced mechanism involving Ti $3d$ states, consistent with a donor exchange mechanism proposed

earlier [19], but with the occupied Ti $3d$ orbitals playing the role of the donors.

The measurements of HAXPES and SX-PES were carried out with the approval of the RIKEN SPring-8 Center (Proposal No. 20090041 and No. 20090033, respectively).

-
- [1] S. A. Wolf *et al.*, Science, **294**, 1488 (2001).
 - [2] Y. Matsumoto *et al.*, Science, **291**, 854 (2001).
 - [3] P. Sharma *et al.*, Nature Mater., **2**, 673 (2003).
 - [4] J. Philip *et al.*, Nature Mater., **5**, 298 (2006).
 - [5] R. Janisch, P. Gopal, and N. A. Spaldin, J. Phys.:Condens. Matter, **17**, R657 (2005).
 - [6] T. Fukumura *et al.*, New J. Phys., **10**, 055018 (2008).
 - [7] H. Munekata *et al.*, Phys. Rev. Lett., **63**, 1849 (1989).
 - [8] D. Chiba, K. Takamura, F. Matsukura, and H. Ohno, Appl. Phys. Lett., **82**, 3020 (2003).
 - [9] S. Kuroda *et al.*, Nature Mater., **6**, 440 (2007).
 - [10] T. Dietl *et al.*, Science, **287**, 1019 (2000).
 - [11] P. Mahadevan, A. Zunger, and D. D. Sarma, Phys. Rev. Lett., **93**, 177201 (2004).
 - [12] D. Kitchen *et al.*, Nature, **442**, 436 (2006).
 - [13] S. R. Shinde *et al.*, Phys. Rev. Lett., **92**, 166601 (2004).
 - [14] J.-Y. Kim *et al.*, Phys. Rev. Lett., **90**, 017401 (2003).
 - [15] J. D. Bryan, S. M. Heald, S. A. Chambers, and D. R. Gamelin, J. Am. Chem. Soc., **126**, 11640 (2004).
 - [16] K. Ueno *et al.*, J. Appl. Phys., **103**, 07D114 (2008).
 - [17] K. Mamiya *et al.*, Appl. Phys. Lett., **89**, 062506 (2006).
 - [18] J. W. Quilty *et al.*, Phys. Rev. Lett., **96**, 027202 (2006).
 - [19] W. Yan *et al.*, Appl. Phys. Lett., **94**, 042508 (2009).
 - [20] J. M. D. Coey, M. Venkatesan, and C. B. Fitzgerald, Nature Mater., **4**, 173 (2005).
 - [21] Y. Takata *et al.*, Nuc. Inst. And Meth. in Phys. Res. A, **547**, 50 (2005).
 - [22] See EPAPS document No. XXXXX for supplementary data.
 - [23] K. Okada, T. Uozumi, and A. Kotani, J. Phys. Soc. Jpn., **63**, 3176 (1994).
 - [24] A. G. Thomas *et al.*, Phys. Rev. B, **75**, 035105 (2007).
 - [25] K. Morikawa *et al.*, Phys. Rev. B, **54**, 8446 (1996).
 - [26] M. Sing *et al.*, Phys. Rev. Lett., **102**, 176805 (2009).
 - [27] J. C. Woicik *et al.*, Phys. Rev. Lett., **89**, 077401 (2002).
 - [28] S. P. Kowalczyk *et al.*, Solid State Commun., **23**, 161 (1977).
 - [29] A. Fujimori *et al.*, Phys. Rev. Lett., **69**, 1796 (1992).
 - [30] H. Sato *et al.*, J. Phys. Soc. Jpn., **75**, 053702 (2006).